

# Nanoscale

Accepted Manuscript



This is an *Accepted Manuscript*, which has been through the Royal Society of Chemistry peer review process and has been accepted for publication.

*Accepted Manuscripts* are published online shortly after acceptance, before technical editing, formatting and proof reading. Using this free service, authors can make their results available to the community, in citable form, before we publish the edited article. We will replace this *Accepted Manuscript* with the edited and formatted *Advance Article* as soon as it is available.

You can find more information about *Accepted Manuscripts* in the [Information for Authors](#).

Please note that technical editing may introduce minor changes to the text and/or graphics, which may alter content. The journal's standard [Terms & Conditions](#) and the [Ethical guidelines](#) still apply. In no event shall the Royal Society of Chemistry be held responsible for any errors or omissions in this *Accepted Manuscript* or any consequences arising from the use of any information it contains.

Cite this: DOI: 10.1039/c0xx00000x

www.rsc.org/xxxxxx

**ARTICLE TYPE**

# Electrospun nanowire-based triboelectric nanogenerator and its application on the full self-powered UV detector

Youbin Zheng,<sup>‡a</sup> Li Cheng,<sup>‡a</sup> Miaomiao Yuan,<sup>a,b</sup> Zhe Wang,<sup>a</sup> Lu Zhang,<sup>a</sup> Yong Qin,<sup>a, c,\*</sup> and Tao Jing<sup>c</sup>*Received (in XXX, XXX) Xth XXXXXXXXXX 20XX, Accepted Xth XXXXXXXXXX 20XX*

DOI: 10.1039/b000000x

A new kind of triboelectric nanogenerator (TENG) is developed based on electrospun PVDF and Nylon nanowires. This nanogenerator exhibits the remarkable characteristics of easy fabrication, low cost and high output. Its open-circuit voltage and short-circuit current density respectively reaches up to 1163 V and 11.5  $\mu\text{A}/\text{cm}^2$  driven by the vibration with the triggering frequency of 5 Hz and the amplitude of 20 mm. The peak power density is 26.6  $\text{W}/\text{m}^2$ . It directly powered a DC motor without an energy storage system for the first time. And by harvesting energy from environment using this TENG, a full self-powered UVR detection device is developed to show the level of UVR directly without additional components.

## Introduction

Over the last few decades, energy crisis has become a global concern and researchers have been making every effort to search for the green and renewable energy source. Harvesting mechanical energy from the environment and biological systems has attracted increasing attention for powering personal electronics. As an emerging technology for mechanical energy harvesting, triboelectric nanogenerators (TENGs) have been recently developed as an effective approach of converting mechanical energy in the environment into electrical energy for self-powered devices and systems by a conjunction of triboelectrification and electrostatic induction.<sup>1-4</sup> It has been demonstrated that the output performance of the TENGs depends intimately on the properties of their materials, such as types<sup>5</sup> and surface structures<sup>6-8</sup> of the materials. Up to now, different preparation methods, such as patterned silicon template made by a complicated procedure<sup>6-9</sup>, typical photolithography process<sup>9</sup> and dry-etching process<sup>10,11</sup>, have been developed to fabricate TENG composed of various materials. But most of these methods are complex and time-consuming, which limits the TENGs' potential applications. From a practical point of view, a highly simple method of the fabrication with superior performance TENG is urgently needed.

On the other hand, although TENGs have been utilized to power sensors to detect mercury ions<sup>12</sup>, pressure<sup>13</sup>, wind vector<sup>14</sup>, active vibration<sup>15</sup> and so on, most of these sensors need to work with the expensive and high-precision electric measurement equipments,<sup>13-16</sup> which will make the sensors hard to be used in some particular situations. Furthermore, the self-powered portable UV detector is beneficial for protecting people from UV light's damage. Up to 60,000 deaths are caused by too much exposure to ultraviolet radiation (UVR) worldwide each year and most of the UV-related illnesses and deaths can be avoided through a series of simple prevention measures, according to the World Health Organization.<sup>17</sup> As more and more people are

aware of the damage of UV exposure for skin, it's greatly significant to design a fully integrated, stand-alone and self-powered UVR level detection device which can display the UVR level anytime and anywhere to alert people to protect their skin when the UV intensity exceeds dangerous limits.

In this work, we developed a new kind of TENG based on electrospun nanowires (ENTENG). It exhibits the remarkable characteristics of easy fabrication, low cost and high output. The open-circuit voltage and the short-circuit current density of the ENTENG respectively reach up to 1163 V and 11.5  $\mu\text{A}/\text{cm}^2$  under the vibration with the triggering frequency of 5 Hz and the amplitude of 20 mm. The peak power density is 26.6  $\text{W}/\text{m}^2$ . When it is driven by human footfalls, we got a peak current density as high as 209  $\mu\text{A}/\text{cm}^2$ . By using this device, we directly powered a DC motor directly without an energy storage system for the first time and developed a full self-powered UVR detection device that could show the level of UVR directly without additional components. This work expands the potential applications of TENGs to the field of public health.

## Results and Discussion

As demonstrated in previous studies, rough surfaces with micro/nano structures have larger effective triboelectric effect and can generate more surface charges during the friction.<sup>6-10,18,19</sup> So in this work we fabricated the nanostructures to enhance the friction and improve the output performance of the TENG by the electrospinning method which is well known as one of the most simple, low-cost and versatile methods for producing nanostructured fibers<sup>20</sup>. The schematic diagram of the ENTENG is shown in Fig. 1a. Poly(vinylidene fluoride) (PVDF) and polyamide (Nylon) are chosen for their high negativity/positivity in the triboelectric series. Ag film electrode and PVDF nanofibers are deposited onto two sides of one Kapton film by magnet sputtering and electrospinning as the top plate, and Ag film electrode and Nylon nanofibers are successively deposited onto the same side of the other Kapton film by the similar method as

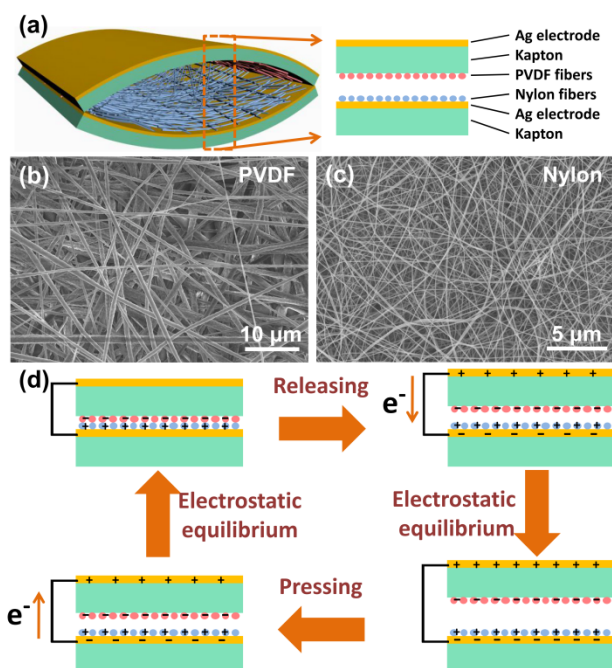


**Fig. 1** Structure and working principle of the ENTENG. (a) Schematic of the ENTENG. (b, c) SEM images of the electrospun PVDF and Nylon nanofibers. (d) The charges distribution in the device and flowing direction in the circuit when the device is pressed and released.

the bottom plate. Owing to the naturally bend of Kapton films, these two processed plates of the same size are attached face-to-face to form the arch-shaped ENTENG (Fig. 1a). The surface morphology of as-spun PVDF and Nylon nanofibers are shown in Fig. 1b and c. The electrospun nanofibers with diameters of approximately 790 nm and 550 nm respectively are randomly distributed on Kapton film. The electricity generation process of the fabricated TENG is schematically depicted in Fig. 1d. When the bending plates are pressed, the top plate and bottom plate contact and rub against each other. As PVDF is much more triboelectrically negative than Nylon, electrons are injected from Nylon to the PVDF surface, generating positive triboelectric charges on the Nylon side and negative charges on the PVDF side. When the ENTENG is being released, the contacting surfaces are separated due to resilience. And the top Ag electrode possesses a lower electric potential than the bottom Ag electrode, producing an electric potential difference<sup>10</sup>, which will drive the electrons to flow through an external load from the top Ag electrode to the bottom Ag electrode to reach an electrostatic equilibrium. In the meantime, positively induced charges are produced on the top Ag electrode and negatively induced charges on the bottom Ag electrode. Once the TENG is pressed again to make the two plates contact, the redistributed charges will build a reversed potential to drive electrons to flow toward the opposite direction. When a new equilibrium is reached, a cycle of electricity generation is finished.

To investigate the electrical output performance of the ENTENG, we use a linear motor to periodically press and release the device. In order to eliminate the influence of the noise caused by the measurement equipment (voltmeter and amperemeter), we changed the way of the device connecting with the measurement

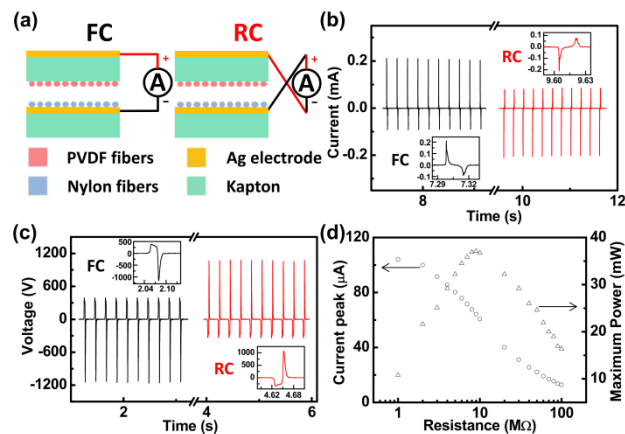


**Fig. 2** Output of the ENTENG. (a) Schematic of forward connection (FC) and reverse connection (RC) which are used to rule out the possible system artifacts. (b, c) Short-circuit current and open-circuit voltage of the ENTENG driven by a linear motor. The black and red curves represent the output signals under FC and RC, respectively. (d) Current (circle) and power (triangle) of the ENTENG with different load resistants.

equipment. As shown in Fig. 2a, the configuration that positive probe of the measurement system connecting with PVDF nanofiber membrane and the negative probe connecting with Nylon nanofiber membrane is defined as forward connection (FC) and the inverted connecting configuration is defined as reverse connection (RC). According to the working principle of the TENG (Fig. 1d), for FC, an instantaneous positive-negative current and voltage will be measured when the TENG is driven by a cyclic pressing-releasing movement of linear motor. Reversely, the negative-positive output current and voltage should be measured for RC. As shown in Fig. 2b and c, driven by the motor's movement with the frequency of 5 Hz and the amplitude of 20 mm, the measured output signals are consistent with above analysis, which means that the output current and voltage are true signals according to the previous work<sup>21</sup>. The short-circuit current (Fig. 2b) and the open-circuit voltage (Fig. 2c) of the ENTENG are 211  $\mu\text{A}$  and 1163 V, respectively. And the corresponding current density is 11.5  $\mu\text{A}/\text{cm}^2$  and the charges flowing between two electrodes per peak are 0.332  $\mu\text{C}$ , giving the corresponding triboelectric charge density of 179.6  $\mu\text{C}/\text{m}^2$ . To investigate the effective electric power of the ENTENG, resistors are connected as external loads. As displayed in Fig. 2d, the instantaneous current drops with increasing load resistance due to Ohmic loss. As a result, the instantaneous power output ( $W=I_{\text{peak}}^2R$ ) reached the maximum value of 37.1 mW at a load resistance of 9 M $\Omega$ , corresponding to a power density of 26.6  $\text{W}/\text{m}^2$ . This result indicates that the ENTENG is particularly efficient when the load has a resistance on the order of  $10^7$  ohms. In addition, the mechanical stability of the ENTENG is investigated. As demonstrated in Fig. S1, only a slight decline (~5%) is observed for the short-circuit current after a total of 36000 working cycles.

To check if the electrospun nanowires are beneficial to the output of TENG, we compared the output of ENTENG with the TENG composed of smooth surfaces (More details are shown in Fig. S2). These two TENGs have the same device structure except that the surface morphology of triboelectric materials is

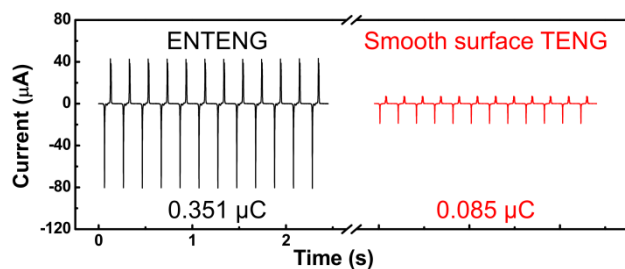


**Fig. 3** The output current of the ENTENG and the output current of the smooth surface TENG with similar device structure.

different. Fig. 3 shows the short-circuit current of TENGs with smooth surface and electrospun nanowire surface measured under the same condition. The short-circuit currents of the ENTENG and the smooth surface TENG are  $81 \mu\text{A}$  and  $19 \mu\text{A}$ , respectively. Meanwhile, the corresponding inductive charges per peak are  $0.351 \mu\text{C}$  and  $0.085 \mu\text{C}$ . There are 4.3 and 4.1 times of increase respectively in short-circuit current and transferred charges. This result shows that the nanowires prepared by electrospinning method is effective in improving the output of TENGs and can compare favorably with that received based on other existing complex preparation methods<sup>6,7</sup>. Therefore, electrospinning benefits to the fabrication of TENG with superior performance and low cost.

To convert the energy of human motion into electricity to power micro/nanosystems, the ENTENG is attached onto a sole to harvest the energy of human walking. Fig. 4a shows that the device produces a peak current of  $3 \text{ mA}$  when driven by human footfalls, which implies that the output current density is  $209 \mu\text{A}/\text{cm}^2$ . By using this ENTENG as a direct power source, we successfully powered a DC motor without energy storage process. The ENTENG is connected to the input end of a bridge rectifier and the DC motor is connected to the output end of the rectifier (Fig. S3). The alternating current obtained from the ENTENG is converted into direct current by the bridge rectifier. As shown in Fig. 4b and Movie 1 in the Supporting Information, the motor began to rotate in clockwise direction when the ENTENG was triggered by hand tapping, and the rotation direction changed to counter clockwise when the DC motor was reversely connected

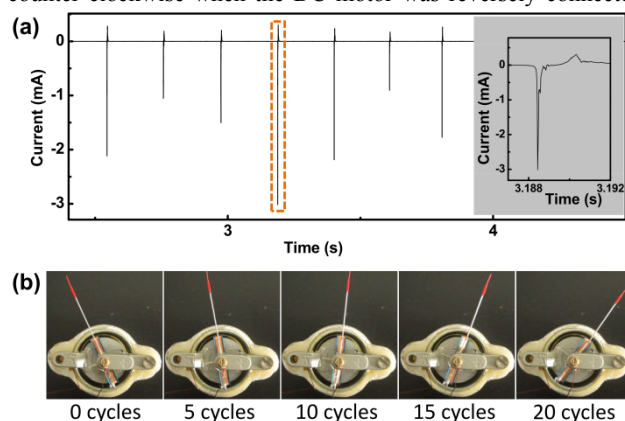


**Fig. 4** Collecting the energy of human motion by the ENTENG. (a) Short-circuit current of the ENTENG triggered by human footfall. The insert shows the details of the highest current peak. (b) Optical images of a DC motor directly driven by hand tapping, which shows the motion of the motor every five working cycles of the ENTENG.

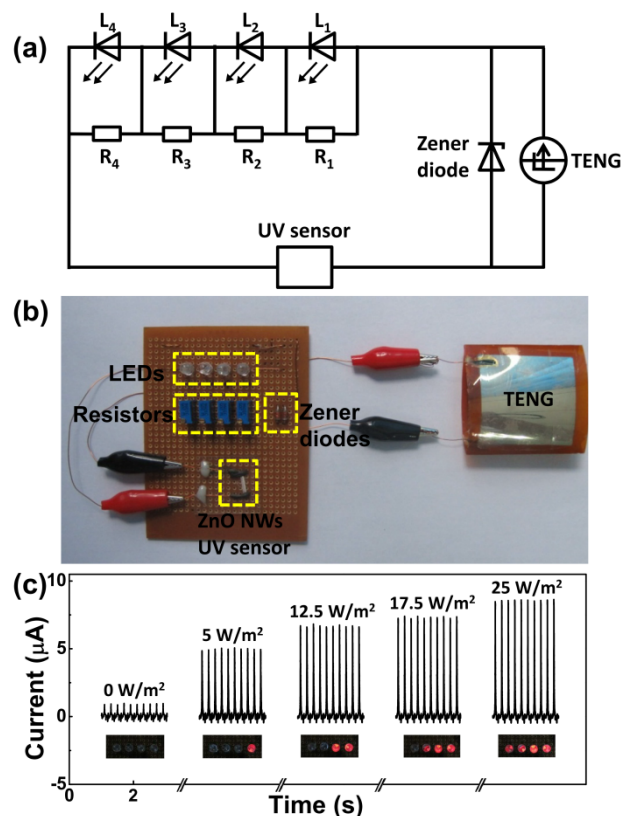


**Fig. 5** A self-powered UVR level detection system driven by the ENTENG. (a, b) Schematic and optical image of the UVR level detection system powered by an ENTENG. (c) Current flowing across the UV sensor and the optical images of the LEDs at UV intensity of  $0, 5, 12.5, 17.5$  and  $25 \text{ W}/\text{m}^2$ .

with the output end of the bridge rectifier. So it feasible to instantaneously drive some commercial DC motors by ENTENG, which expands the application of triboelectric nanogenerator.

As the output current of the ENTENG changes with the loads of different resistance, it is possible to integrate the ENTENG with a UV sensor to fabricate a self-powered UVR level detection device to detect the UVR level of low, moderate, high, very high and extreme defined by World Health Organization<sup>21</sup>. As shown in Fig. 5a and b, an ENTENG is connected in series with a ZnO nanofiber based UV sensor and four LEDs, while shunt resistors are connected in parallel with each LED. The resistances we used are  $96.3, 30.6, 22.5$  and  $17.2 \text{ k}\Omega$ , corresponding to  $R_1, R_2, R_3$  and  $R_4$ , respectively. A series of Zener diodes with the reverse breakdown voltage of  $182 \text{ V}$  are connected in parallel with the TENG, which are used to provide a stable working voltage and prevent damage to electronics. In this experiment, we tried to automatically warn the five UVR levels by the boundary values of  $5, 12.5, 17.5$  and  $25 \text{ W}/\text{m}^2$ . From the current-time curve of the UV sensor under  $1 \text{ V}$  bias voltage and different UV light intensities shown in Fig. S4, the resistance of the UV sensor changes with the light intensity, which results in the change of the current according to Ohm's law. When the UV intensity is higher than the boundary value of different UVR levels, the LED begins to flicker. In this way, the UVR level could be displayed by the number of flickering LEDs. When the UV intensity is less than  $5 \text{ W}/\text{m}^2$ , the UV sensor has a very high resistance and the current in the circuit is so small that no LED flickers, which means low

danger from the UV light. When the UV intensity reaches or exceeds 5 W/m<sup>2</sup> but less than 12.5 W/m<sup>2</sup>, the resistance of UV sensor decreases because of the increasing carriers so that the corresponding current is increased and one LED flickers, which means moderate risk of harm from unprotected UV exposure. With the increasing of UV intensity, more carriers are generated in the ZnO nanowires. So two LEDs flicker which means high risk of harm when the UV intensity is in the range of 12.5 W/m<sup>2</sup> to 17.5 W/m<sup>2</sup>. Analogously, three LEDs flicker means very high risk of harm (17.5 to 25 W/m<sup>2</sup>), and four LEDs flicker means extreme risk of harm (more than 25 W/m<sup>2</sup>). Fig. 5c shows the optical images of the LEDs and the output current of the ENTENG in the circuit at the UV intensity of 0, 5, 12.5, 17.5 and 25 W/m<sup>2</sup>. More details are illustrated in Supporting Information Movie 2. As shown above, the UVR level detection device is very simple and easy to be integrated with the self-powered portable equipment. By using this equipment, anyone can measure the UVR level anytime and take proper steps to protect his skin and eyes. This work not only presents a portable and self-powered UVR level detection device to alert people to a possible over-exposure to UV light, but also expands the applicability of TENGs as power sources for self-sustained electronics.

## Conclusions

In summary, based on electrospinning method, we developed a new way to fabricate the high performance TENG. The ENTENG exhibits the remarkable characteristics of easy fabrication, low cost and high output. Driven by a linear motor at the frequency of 5 Hz and the amplitude of 20 mm, we got a short-circuit current density of 11.5 μA/cm<sup>2</sup> and an open-circuit voltage of 1163 V. The peak power density is 26.6 W/m<sup>2</sup>. Attached onto the sole to collect energy of human motion, the ENTENG produced the highest peak current density of 209 μA/cm<sup>2</sup> when driven by human footfalls. Moreover, the ENTENG is successfully used to power a DC motor directly by collecting the energy of hand tapping. And by using the ENTENG as a power source, we fabricated a full self-powered and portable UVR level detection device which could measure and display the UVR level directly. This work unambiguously shows the feasibility of ENTENG for powering portable sensors for health care and other electronic devices.

## Experimental Section

### Preparation of the PVDF and Nylon solutions

3.75 g PVDF was mixed with 8.5 g N,N-dimethylacetamide (DMAC) and 12.75 g acetone in a 50 mL triangular flask. The solution was stirred at 60 °C for 30 min and cooled to room temperature. 2 g Nylon was mixed with 4.8 g formic acid and 3.2 g dichloromethane in a 50 mL triangular flask, then it was stirred for 1 h to ensure the dissolution of Nylon. All reagents were analytically pure and used without any further purification.

### Preparation of PVDF and Nylon nanofiber

The experimental setup of electrospinning to fabricate the nanofibers is a horizontal electrospinning setup reported in previous works<sup>22</sup>. The solution is loaded into a syringe and the

distance between the needle and the collector is 16 cm for all the experiments. To prepare PVDF nanofibers, electrospinning is conducted at 15 kV with the feed rate of PVDF solution 3 mL/h. For Nylon, the applied electrospinning voltage is 16 kV and the Nylon solution feed rate is 1 mL/h. All the nanofibers are collected on Kapton substrates for 10 min. The samples obtained after electrospinning are dried at 60 °C for 30 min in a ventilated oven.

### Fabrication of the ZnO nanofiber based UV Sensor

The ZnO precursor is prepared by using a reported method<sup>23</sup>. With a vertical electrospinning setup, electrospinning is conducted at 25 kV and the distance between the needle and the collector is 20 cm. The as-electrospun nanowires are calcined at 450 °C in air for 3 h. The heating rate is 2 °C/min. The two ends of the as-prepared ZnO nanowires are connected with carbon electrodes without any package to make the UV sensor.

### Acknowledgements

We gratefully acknowledge the financial support from NSFC (NO. 51322203), Fok Ying Tung education foundation (NO. 131044), PCSIRT (NO. IRT1251), the "thousands talents" program for pioneer researcher and his innovation team, China, the Fundamental Research Funds for the Central Universities (No. lzujbky-2013-k04, lzujbky-2013-34, lzujbky-2013-230).

### Notes and references

- <sup>a</sup> Institute of Nanoscience and Nanotechnology, Lanzhou University, Lanzhou, 730000, China. E-mail: qinyong@lzu.edu.cn
- <sup>b</sup> The Research Institute of Biomedical Nanotechnology, Lanzhou University, Lanzhou, 730000, China.
- <sup>c</sup> Beijing Institute of Nanoenergy and Nanosystems, Chinese Academy of Sciences, Beijing 100085, China.
- † Electronic Supplementary Information (ESI) available. See DOI:10.1039/b000000x/
- ‡ These authors contributed equally to this work.
- Z. L. Wang, *Acs Nano*, 2013, **7**, 9533.
- Z. H. Lin, G. Cheng, L. Lin, S. Lee and Z. L. Wang, *Angewandte Chemie-International Edition*, 2013, **52**, 12545.
- W. Q. Yang, J. Chen, G. Zhu, J. Yang, P. Bai, Y. J. Su, Q. S. Jing, X. Cao and Z. L. Wang, *Acs Nano*, 2013, **7**, 11317.
- Y. J. Su, Y. Yang, H. L. Zhang, Y. N. Xie, Z. M. Wu, Y. D. Jiang, N. Fukata, Y. Bando and Z. L. Wang, *Nanotechnology*, 2013, **24**, 295401.
- F. R. Fan, Z. Q. Tian and Z. L. Wang, *Nano Energy*, 2012, **1**, 328.
- F. R. Fan, L. Lin, G. Zhu, W. Z. Wu, R. Zhang and Z. L. Wang, *Nano Letters*, 2012, **12**, 3109.
- X. S. Zhang, M. D. Han, R. X. Wang, F. Y. Zhu, Z. H. Li, W. Wang and H. X. Zhang, *Nano Letters*, 2013, **13**, 1168.
- M. D. Han, X. S. Zhang, B. Meng, W. Liu, W. Tang, X. M. Sun, W. Wang and H. X. Zhang, *Acs Nano*, 2013, **7**, 8554.
- S. H. Wang, L. Lin and Z. L. Wang, *Nano Letters*, 2012, **12**, 6339.
- G. Zhu, C. F. Pan, W. X. Guo, C. Y. Chen, Y. S. Zhou, R. M. Yu and Z. L. Wang, *Nano Letters*, 2012, **12**, 4960.
- L. Lin, S. H. Wang, Y. N. Xie, Q. S. Jing, S. M. Niu, Y. F. Hu and Z. L. Wang, *Nano Letters*, 2013, **13**, 2916.
- Z. H. Lin, G. Zhu, Y. S. Zhou, Y. Yang, P. Bai, J. Chen and Z. L. Wang, *Angewandte Chemie-International Edition*, 2013, **52**, 5065.
- L. Lin, Y. N. Xie, S. H. Wang, W. Z. Wu, S. M. Niu, X. N. Wen and Z. L. Wang, *Acs Nano*, 2013, **7**, 8266.
- Y. Yang, G. Zhu, H. L. Zhang, J. Chen, X. D. Zhong, Z. H. Lin, Y. J. Su, P. Bai, X. N. Wen and Z. L. Wang, *Acs Nano*, 2013, **7**, 9461.

- 15 J. Chen, G. Zhu, W. Q. Yang, Q. S. Jing, P. Bai, Y. Yang, T. C. Hou and Z. L. Wang, *Advanced Materials*, 2013, **25**, 6094.
- 16 Y. Yang, H. L. Zhang, Z. H. Lin, Y. S. Zhou, Q. S. Jing, Y. J. Su, J. Yang, J. Chen, C. G. Hu and Z. L. Wang, *Acs Nano*, 2013, **7**, 9213.
- 5 17 R. Lucas, T. McMichael, W. Smith and B. Armstrong, *Solar Ultraviolet Radiation: Global burden of disease from solar ultraviolet radiation*, Report No. 13, World Health Organization, Geneva, 2006.
- 18 P. Bai, G. Zhu, Z. H. Lin, Q. S. Jing, J. Chen, G. Zhang, J. Ma and Z.  
10 L. Wang, *Acs Nano*, 2013, **7**, 3713.
- 19 G. Zhu, Z. H. Lin, Q. S. Jing, P. Bai, C. F. Pan, Y. Yang, Y. S. Zhou and Z. L. Wang, *Nano Letters*, 2013, **13**, 847.
- 20 D. Li and Y. N. Xia, *Advanced Materials*, 2004, **16**, 1151.
- 21 R. S. Yang, Y. Qin, C. Li, L. M. Dai and Z. L. Wang, *Applied  
15 Physics Letters*, 2009, **94**, 022905.
- 22 World Health Organization, *Global Solar UV Index: A Practical Guide*, WHO, Geneva, Switzerland, 2002.
- 23 G. G. Li, Z. Y. Hou, C. Peng, W. X. Wang, Z. Y. Cheng, C. X. Li, H. Z. Lian and J. Lin, *Advanced Functional Materials*, 2010, **20**, 3446.
- 20 24 Z. T. Zhu, L. F. Zhang, J. Y. Howe, Y. L. Liao, J. T. Speidel, S. Smith and H. Fong, *Chemical Communications*, 2009, 2568.